ACS APPLIED MATERIALS & INTERFACES

www.acsami.org

Research Article

Covalently Attached Slippery Surface Coatings to Reduce Protein Adsorptions on Poly(dimethylsiloxane) Planar Surfaces and 3D Microfluidic Channels

Yue Cao,[†] Xingchi Chen,[†] Avi Matarasso, Zizheng Wang, Yang Song, Guangfu Wu, Xincheng Zhang, He Sun, Xueju Wang, Michael R. Bruchas, Yan Li,* and Yi Zhang*

Cite This: *ACS Appl. Mater. Interfaces* 2023, 15, 9987−9995

Read Online

ACCESS | Metrics & More | Article Recommendations | Supporting Information

ABSTRACT: Silicone elastomers, such as poly(dimethylsiloxane) (PDMS), have a broad range of applications in basic biomedical research and clinical medicine, ranging from the preparation of microfluidic devices for organs-on-chips and ventriculoperitoneal shunts for the treatment of hydrocephalus to implantable neural probes for neuropharmacology. Despite the importance, the protein adsorptions on silicone elastomers in these application environments represent a significant challenge. Surface coatings with slippery lubricants, inspired by the *Nepenthes* pitcher plants, have recently received much attention for reducing protein adsorptions. Nevertheless, the depletion of the physically infused lubricants limits their broad applications. In this study, we report a covalently attached slippery surface coating to reduce protein adsorptions on PDMS surfaces. As demonstrations, we show that the adsorption of serum proteins, human fibrinogen and albumin, can be significantly reduced by the slippery surface coating in both planar PDMS surfaces and 3D microfluidic channels. The preparation of slippery surface coatings relies on the acid-catalyzed polycondensation reaction of dimethyldimethoxysilane, which utilizes a low-cost and scalable dip-coating method. Furthermore, cell metabolic activity and viability studies demonstrate the biocompatibility of the surface coating. These results suggest the potential applications of slippery surface coatings to reduce protein adsorptions for implantable medical devices, organs-on-chips, and many others.

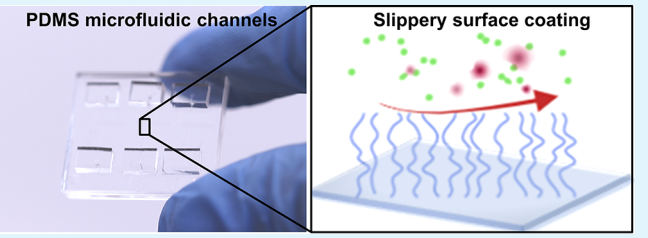

KEYWORDS: *slippery surface coatings, PDMS, planar surfaces, 3D microfluidic channels, protein adsorptions*

INTRODUCTION

Silicone elastomers, such as poly(dimethylsiloxane) (PDMS), have been widely used in the preparation of many clinically approved medical devices,[1] including breast implants,[2] dialysis membranes,[3] intraocular lenses,[4,5] and many others. Because of their material biocompatibility, tissue-like mechanical property (∼1 MPa), and optical transparency, they are also frequently used in the emerging field of bioelectronics and biosensors, such as in microfluidics for tissue engineering,[6] wearable electronics for sweat samplings,[7−9] and implantable neural probes for neuropharmacology and neurochemical sampling.[10−12] Despite these attractive properties of PDMS-based materials and their wide range of applications, the nonspecific protein adsorptions and resulting biofouling represent a significant challenge for these applications. For example, the protein adsorptions and immune response could block the microchannels of implantable microfluidics for drug delivery,[10−12] resulting in device failure and replacement. Similarly, protein adsorption on the PDMS encapsulation layers of implantable optogenetic devices could reduce the output intensity of the microscale light-emitting diodes. Additionally, for implantable neural probes that are coated with PDMS layers, damage of the brain neurovascular unit during probe implantation often causes the release of proinflammatory and neurotoxic serum proteins, such as fibrinogen and albumin, into the surrounding brain tissues.[13] These released proteins adsorb on the PDMS surface and promote the adhesion of microglia, thereby triggering a series of inflammatory immune responses and the formation of glial scars on the implant surfaces. These formed scars can encapsulate the implant surface and cause recording/stimulation performance degradation over time.[14]

To solve this issue, various surface coatings have been developed to minimize protein adsorption and biofouling at material's surfaces (Table S1),[15,16] including PDMS. Poly(ethylene glycol) (PEG) and its derivatives are the gold-standard protein-resistant surface coatings for implantable

Received: November 19, 2022
Accepted: January 26, 2023
Published: February 10, 2023

https://doi.org/10.1021/acsami.2c20834
ACS Appl. Mater. Interfaces 2023, 15, 9987−9995

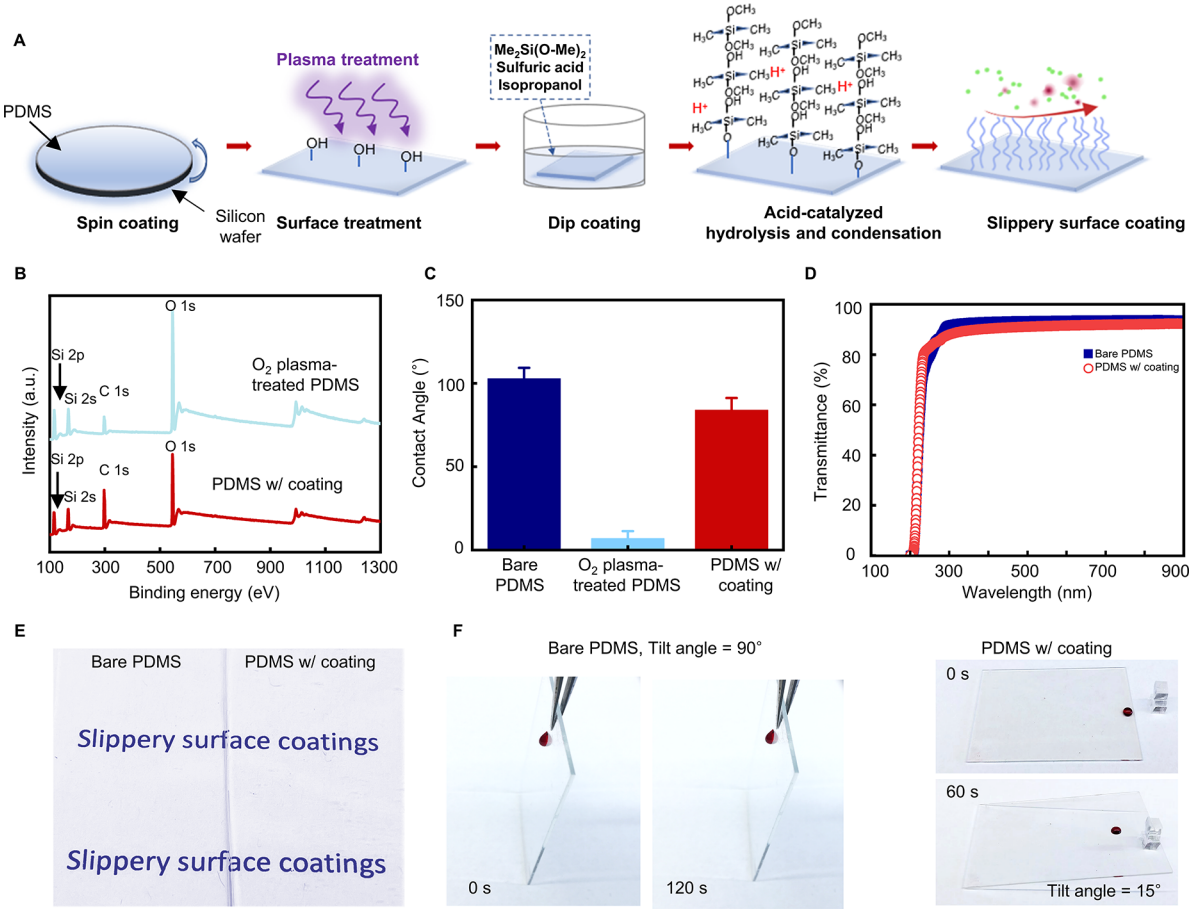

Figure 1. Preparation and characterization of the slippery surface coating. (A) Schematic illustration for the preparation of the surface coating based on the acid-catalyzed polycondensation reaction of dimethyldimethoxysilane. (B) XPS spectra of oxygen plasma-treated PDMS with and without the surface coating. (C) Static water contact angles on PDMS surfaces, oxygen plasma-treated PDMS surfaces, and surfaces with coatings. n = 5. (D) UV−Vis spectra of PDMS thin films with and without the slippery surface coating. (E) White paper with printed words "slippery surface coatings" covered by PDMS thin films with and without the surface coating. (F) The mobility of water droplets (with red dye) on PDMS surfaces with and without the surface coating.

devices.[17] Nevertheless, PEG gel suffers from hydrolysis and oxidative degradation and enzymatic cleavage during *in vivo* applications.[18,19] Recently, zwitterionic polymers have been demonstrated to have exceptional antibiofouling properties,[20−22] although they still face reduced stability in long-term operations due to the presence of the hydrolysis ester group.[23]

Slippery liquid-infused porous surfaces, inspired by the *Nepenthes* pitcher plants, have recently received much attention for various biomedical applications.[24−27] A recent study showed that a lubricant-infused neural probe significantly reduces the insertion damage and foreign-body response.[28] Nevertheless, the lubricant depletion during the insertion represents a significant challenge because of the physically infused lubricant layer (lack of covalent bonding).[29−31] The lubricant depletion issue could be resolved by covalently grafting "liquid-like" polymer brushes onto the surface. Wu et al. reported a slippery "liquid-like" surface for antibiofouling applications via thermally activated equilibration reactions of methoxy-terminated polydimethylsiloxane (PDMS-OCH_3).[32] Nevertheless, the relatively high temperature (120 °C) and lengthy preparation time (24 h) could cause damage to the underlying bioelectronics, thereby limiting its broader applications. Different from the thermally activated reactions, the "liquid-like" polymer brushes can be prepared by the acid-catalyzed polycondensation reaction of dimethyldimethoxysilane,[33] which is time-efficient and can be operated at room temperature. Nonetheless, there have not been any studies to report whether this surface coating can be used to reduce protein adsorptions on planar PDMS surfaces and 3D microfluidic channels.

Here, we report that covalently attached slippery surface coatings can significantly reduce the protein adsorptions on planar PDMS surfaces and in microfluidic channels by using human fibrinogen and albumin as two model serum proteins. Additionally, upon interaction with induced neural progenitor cells (iNPCs), these surface coatings are capable of coculturing with iNPCs in a long-term culture. We also confirm that iNPC cultures containing such coatings show good cell viability compared with the cell-only control group. The optical transparency, low-cost operation, scalable manufacturing, antiprotein adsorption property, and biocompatibility illustrate the potentially wide range of applications ranging from implantable medical devices to wearable sensors.

RESULTS AND DISCUSSION

Preparation and Characterization of Slippery Surface Coatings. Slippery surface coatings are prepared by the acid-catalyzed polycondensation reaction of dimethyldimethoxysi-

https://doi.org/10.1021/acsami.2c20834
ACS Appl. Mater. Interfaces 2023, 15, 9987−9995

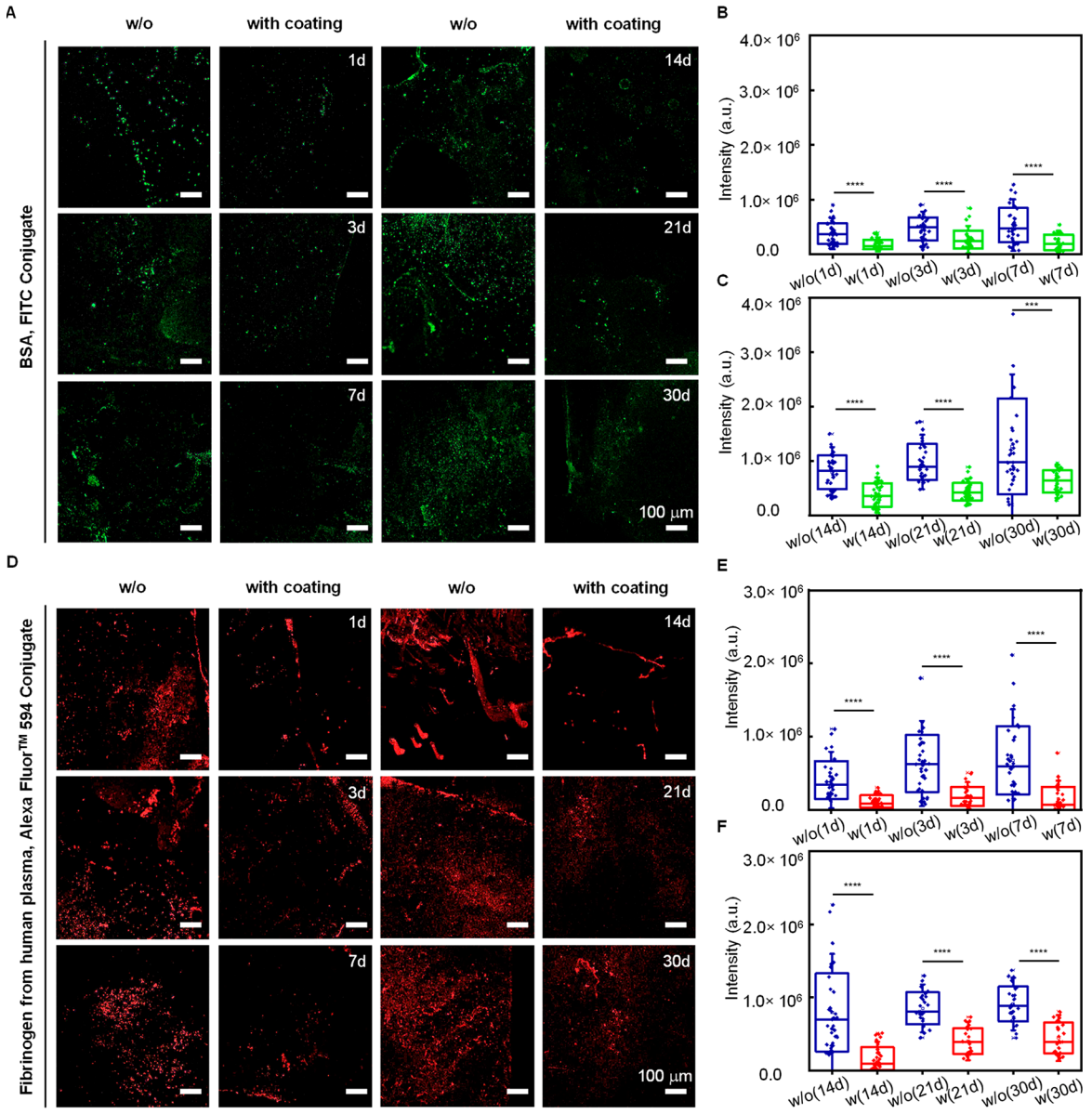

Figure 2. Antiprotein adsorption property of planar PDMS surfaces with and without slippery coatings. (A) Representative confocal fluorescence microscopy images and (B and C) quantitative analysis of the average intensity of planar PDMS thin films without (control) and with a slippery coating incubated in 1 mg/mL BSA−FITC conjugates (green) for 1, 3, 7, 14, 21, and 30 days (****, $P < 0.0001$; ***, $P < 0.001$). (D) Representative confocal fluorescence microscopy images and (E and F) quantitative analysis of the average intensity of planar PDMS surfaces with and without slippery surface coatings incubated in 1 mg/mL fibrinogen Alexa Fluor 594 conjugates for different days (****, $P < 0.0001$). Data are displayed with mean ± standard deviation values. Statistical significance is evaluated by Student's t tests.

lane because of their simple operation procedures and scalability, thereby enabling future distribution to the broad end-user community. Briefly, the preparation of slippery surface coatings starts with an oxygen plasma treatment of the PDMS surfaces (to generate hydroxyl groups), followed by dip-coating the surface in an isopropyl alcohol solution containing dimethyldimethoxysilane and sulfuric acid for ∼30−60 s and drying at room temperature or in a 75 °C oven (Figure 1A). During the drying step, PDMS brushes are rapidly grafted onto the surfaces due to acid-catalyzed hydrolysis and condensation of dimethyldimethoxysilane.[33] As a result, one end of the formed surface coating (PDMS brush) is covalently attached to the surface through a Si−O bond (Figure 1A), while the remaining part of the PDMS brush shows high mobility. To support the formation of the surface coating, X-ray photoelectron spectroscopy (XPS) spectra of the PDMS surfaces before and after the surface coating are shown in Figures 1B and S1. From the high-resolution spectra, characteristic peaks, including O 1s, C 1s, Si 2s, and Si 2p, are observed. For oxygen-plasma-treated PDMS surfaces, the hydroxyl groups are generated on the PDMS surface, and thus a high O 1s peak is observed. After the surface coating, an increase of carbon/oxygen ratio is observed, indicating the successful grafting of PDMS brushes on oxygen-plasma-treated surfaces. It should be noted that the XPS measurement of grafted PDMS brushes may be interfered with by the underlying substrates. To that end, we further confirm the formation of the surface coating by conducting contact-angle (CA) measurements. Figure 1C compares the wetting properties of the PDMS surfaces before and after the surface

https://doi.org/10.1021/acsami.2c20834
ACS Appl. Mater. Interfaces 2023, 15, 9987−9995

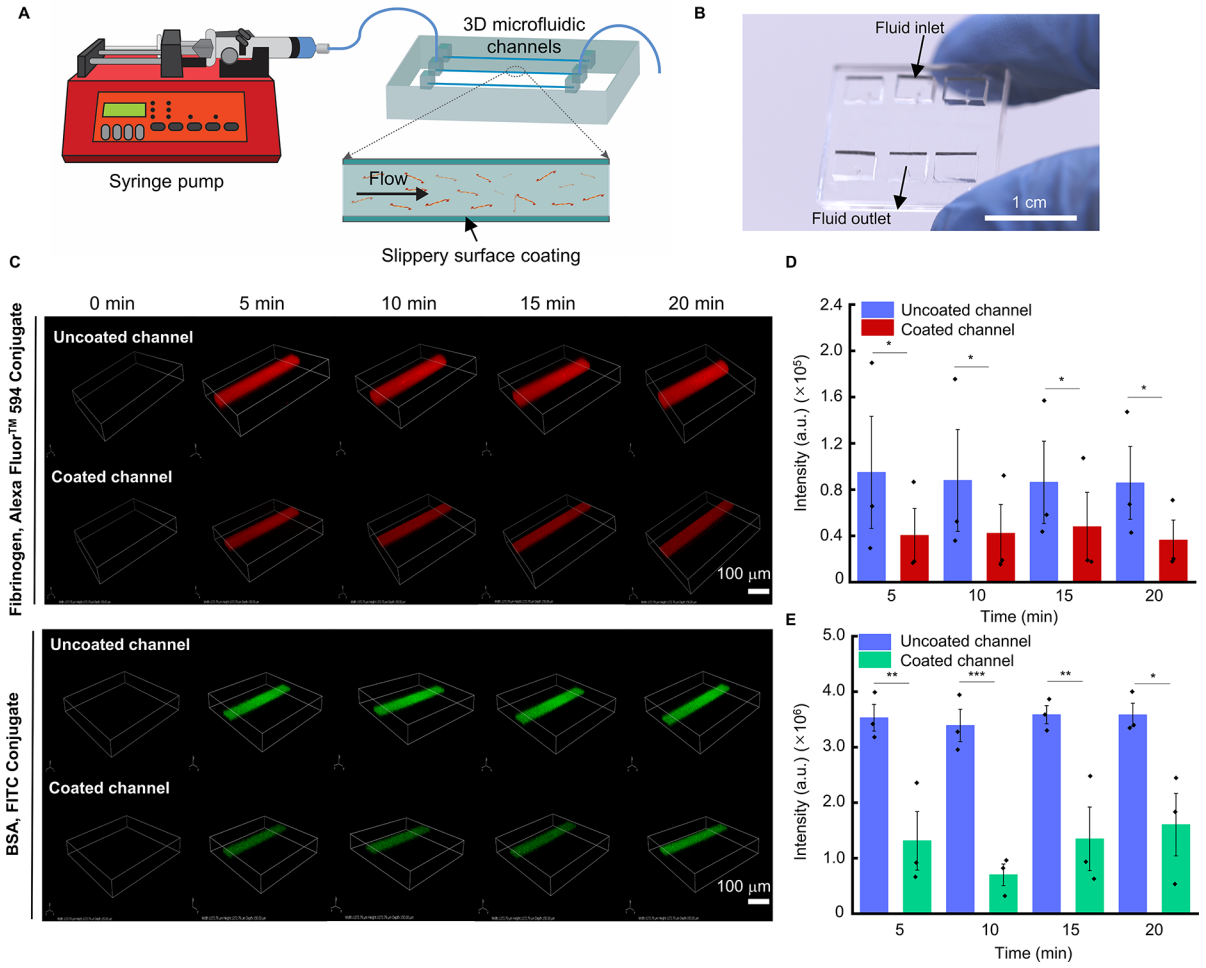

Figure 3. Antiprotein adsorption property on 3D PDMS microfluidic channels. (A) Schematic illustration of the setup to evaluate the antiprotein adsorption property in PDMS microfluidic channels. (B) Optical image of a representative microfluidic device. (C) 3D mapping confocal fluorescence images of 3D microfluidic channels with and without slippery surface coatings infused with fibrinogen (red) and BSA−FITC (green) solutions. (D and E) Quantitative analysis of the average fluorescence intensity as a function of time for microfluidic channels with and without surface coatings. $n = 3$. Data are displayed with mean ± standard deviation values (*, $P < 0.05$; **, $P < 0.01$; ***, $P < 0.001$). Statistical analysis is performed by Student's t tests.

coating presented by the quantitative analysis of static water CAs measured using a tensiometer (Data physics OCA). The pristine PDMS surfaces exhibit hydrophobic characteristics with a high water CA ($\theta = 102.8 \pm 4.3°$), while oxygen-plasma-treated PDMS surfaces present a strong affinity with water, leading to a low water CA ($\theta = 7.0 \pm 2.9°$) due to the formation of the hydroxyl groups (−OH). A significant increase in the CA ($\theta = 84.0 \pm 4.8°$) is observed after the surface coating, indicating the successful grafting of the surface coating. Importantly, this wettability change before and after the surface coating could be used as a simple visual inspection to examine whether these coatings have been successfully attached on the surface (Figures 1C and S2).

The optical property of the surface coating is critical for implantable optoelectronics, such as optical fibers for optogenetics and photometry.[34] Figure 1D shows the optical transmittance spectra of a surface without coating (control) and with the slippery surface coating. PDMS with the slippery surface coating maintains its superior transparency (~90%) in the visible-wavelength range. Figure 1E shows optical images of a covalently attached slippery surface coating on top of a white paper with printed words of "slippery surface coatings", demonstrating the optical transparency of the surface coating. The covalently attached PDMS brushes show "liquid-like" properties due to their ultralow glass transition temperature ($T_g = -125$ °C) and excellent slippery properties toward both nonpolar and polar liquids.[33] To test the slippery properties of the surface coating, we measure the mobility of water droplets on PDMS surfaces with and without the slippery coating (Figure 1F and Movies S1 and S2). For PDMS without the surface coating, the water droplet does not slide even when the substrates are placed vertically for 120 s. In contrast, when a water droplet is placed on the surface with the surface coating, it slides freely from the right to left side at a tilting angle of 15°, without any visible wetting trails. Furthermore, the speed-dependent friction coefficients are measured under a constant load force of 1 N (Figure S3). A significant reduction in the coefficient of friction is observed for PDMS surfaces after the slippery surface coatings, which is attributed to the formation of covalently attached, highly mobile PDMS brushes on the surface.

Antiprotein Adsorption Property on Planar PDMS Surfaces. We evaluate the antiprotein adsorption property of the covalently attached slippery surface coating by using fluorescein-conjugated bovine serum albumin (BSA−FITC conjugate) as a model serum protein. Briefly, PDMS thin films

https://doi.org/10.1021/acsami.2c20834
ACS Appl. Mater. Interfaces 2023, 15, 9987−9995

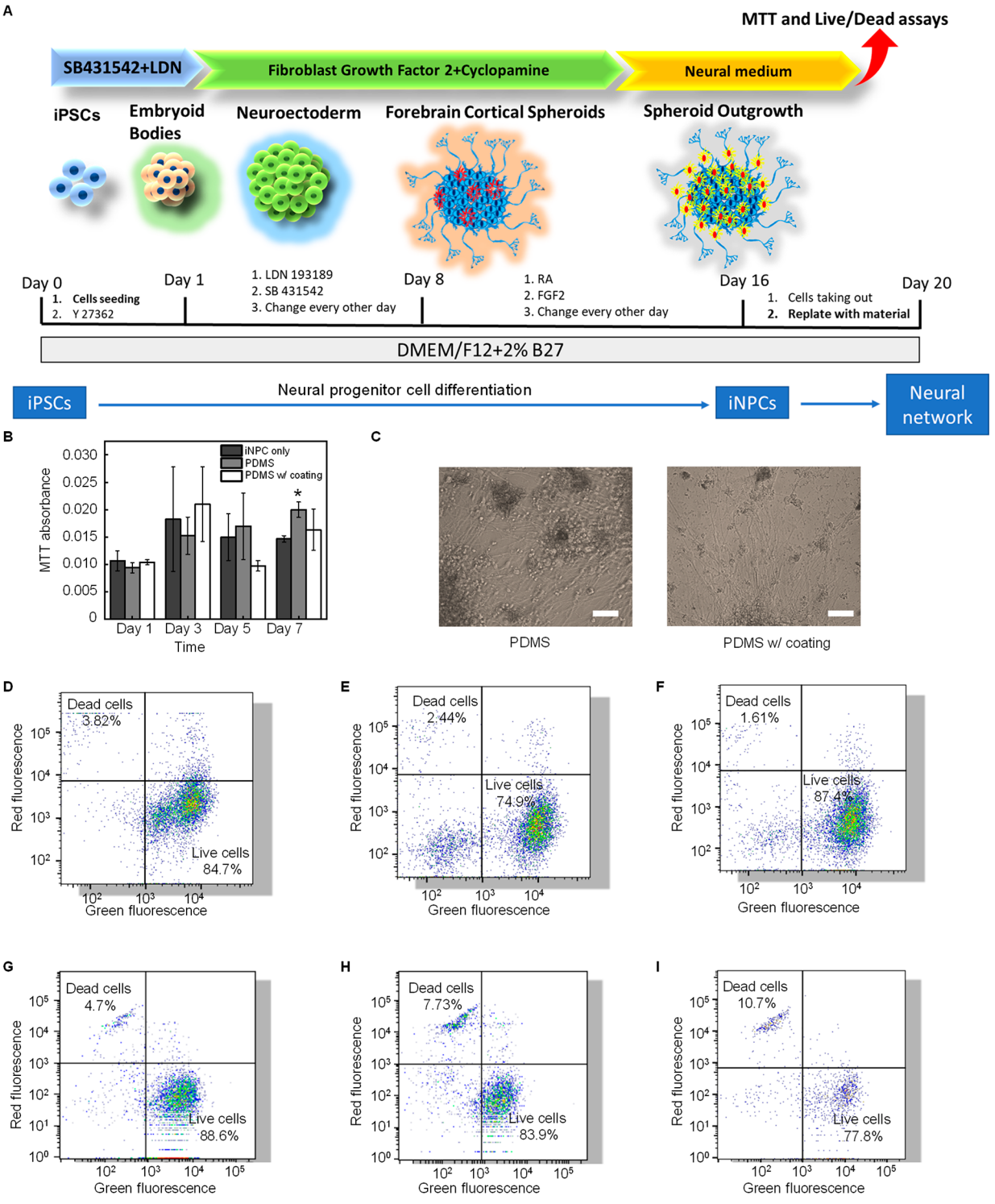

Figure 4. Biocompatibility test of the slippery surface coating coculture system with iNPCs. (A) Timeline of cortical spheroid and iNPC derivation from hiPSC and the coculture. (B) MTT activity of iNPCs cocultured with a biofilm. Statistical analysis was conducted by ANOVA with Tukey's test (n = 4). It should be noted that the iNPC only group has a significant difference with the bare PDMS group but not with the PDMS with the coating group. (C) iNPC morphology showing the occurrence of a neural network after 10 days of replating and coculturing with PDMS and PDMS with the slippery surface coating, respectively. Scale bar = 100 μm. (D–F) Flow cytometry plots of live/dead assay for short-term culture (7 days) with cell only, PDMS with coating, and bare PDMS, respectively. (G–I) Flow cytometry plots of live/dead assay for long-term culture (21 days) with cell only, PDMS with coating, and bare PDMS, respectively. Green fluorescence indicates the live cell population, and red fluorescence indicates the dead cell population.

with and without slippery surface coatings are incubated in a 1× phosphate-buffered saline (PBS) with a protein concentration of 1 mg/mL at 37 °C for 1, 3, and 7 days. As shown in the confocal fluorescence microscopy images (green: BSA) in Figure 2A and the quantitative average intensity (Figure 2B), many proteins are observed on the surface without the coating

https://doi.org/10.1021/acsami.2c20834
ACS Appl. Mater. Interfaces 2023, 15, 9987−9995

as soon as 1 day after incubation. In contrast, significantly reduced adsorption (42−59% reduction) of BSA is observed when the slippery surface coating is applied (Figure 2B and Table S2), mainly because of the slippery "liquid-like" property of its covalently attached PDMS brushes, which can prevent the adsorption of proteins. In long-term studies, the antiprotein adsorption property of the slippery surface coating is further proven by incubating PDMS thin films with and without the coating for 14, 21, and 30 days (Figure 2C and Table S2). The mechanical stability is critical for practical applications. To that end, we investigate the mechanical durability of a covalently attached slippery surface coating by stretching at a 5% strain 10,000 times or stirring in 1× PBS at 500 rpm for 3 days (Figure S4A,B). The confocal fluorescence microscopy images (Figure S4C) and quantitative average intensity characterizations (Figures S4D−F) suggest that PDMS thin films with slippery surface coatings maintain the capability to significantly reduce the protein adsorptions after mechanical deformations by stretching and stirring (****,$P < 0.0001$; ***, $P < 0.001$). The antiprotein adsorption property of the slippery surface coating was further proven by incubating PDMS with and without the coating in 1 mg/mL fibrinogen (human fibrinogen Alexa Fluor 594 conjugates) for 1, 3, 7, 14, 21, and 30 days (Figure 2D−F and Table S2).

Antiprotein Adsorption Property on 3D PDMS Microfluidic Channels. Inspired by the significant reduction of protein adsorptions with the slippery surface coating on planar PDMS surfaces, we then wonder whether such coatings could be adapted to 3D microfluidic channels because microfluidic channels have multiple applications ranging from implantable neural probes for drug delivery to platforms for organs-on-chips.[35] To answer this question, we studied the antiprotein adsorption property on 3D PDMS microfluidic channels. Figure 3A shows a schematic illustration of the setup, including a syringe pump, a microsyringe that contains protein-rich solutions, and 3D microfluidic channels with liquid-like surface coatings. Figure 3B shows an optical image of a PDMS device with multiple 3D microfluidic channels. The protein-rich solution (1 mg/mL human fibrinogen or BSA) is infused through microfluidic channels with a flow rate of 1 μL/min by using a syringe pump. 3D mapping images that incorporate the whole depths of microfluidic channels from the bottom to top layers as a function of time are shown in Figure 3C. Fibrinogens (red fluorescence) are observed in microfluidic channels without surface coatings. The fluorescence intensity increases significantly from 0 to 5 min and reaches a plateau from 5 to 20 min. In contrast, microfluidic channels with slippery coatings show reduced fluorescence signals (Figure 3C). Quantitative analysis of the fluorescence intensity using *ImageJ* software further confirms the reduced protein adsorptions (55−79% reduction for BSA and 44−57% reduction for fibrinogen) for 3D microfluidic channels with surface coatings (Figure 3D,E and Table S3) mainly because highly mobile PDMS brushes attached on the channel surfaces prevent the protein adsorptions. To further evaluate the effective cleaning of surface coatings on the microfluidic channels, we also performed related experiments using deionized (DI) water to flush through the microfluidic channel after emptying the protein solution. Figure S5 shows the changes in the fluorescence intensity as a function of time for effective cleaning. With slippery-surface-coated microfluidic channels, the proteins were easily and quickly removed, resulting in a significant decrease in the intensity signal as soon as 1 min. In contrast, with uncoated microfluidic channels, the protein remained attached to the surface of the microfluidic channels and a much smaller decrease in the fluorescence intensity was observed. Overall, this study suggests the effective cleaning of 3D PDMS microfluidic channels using slippery surface coatings.

Cell Metabolic Activity Determined by MTT Assay. Biocompatibility is a key consideration for *in vivo* applications of the developed surface coatings, which determines how long and how well they are capable of sustaining their functionality in the physiological environment. Human cortical spheroid or organoid models have emerged as a promising platform for neurotoxicity, drug screening, and disease modeling studies.[36,37] Our previous study has investigated the interactions of cortical spheroids with various biomaterials, including nanoparticles and microplastics.[38] The timeline of cortical spheroid formation and iNPC development from human-induced pluripotent stem cells (hiPSCs) is shown in Figure 4A. MTT activity shows the cell viability and metabolic activity observed over 1, 3, 5, and 7 days for bare PDMS and PDMS with the slippery surface coating in the coculture systems in comparison with the cell-only group (Figure 4B). With increasing culture time, the activity of iNPCs increased and reached a plateau. iNPC morphology shows the occurrence of a neural network after 10 days of replating and coculturing with PDMS and with slippery surface coatings, respectively (Figure 4C). These results indicate that the biocompatibility of the slippery surface coatings with iNPCs is comparable with that of the cell-only group.

Cell Viability Determined by Live and Dead Flow Cytometry Assay. For the biocompatibility of slippery surface coatings with iNPCs of the cortical spheroids, there are two different types of experiments conducted: a short-term 7-day coculture and a long-term 21-day coculture. The cell viabilities are measured by live/dead assay quantified by flow cytometry. The short-term culture data are shown in parts D−F of Figure 4, and the long-term culture data are shown in parts G−I of Figure 4. For short-term culture, the live cells in PDMS with slippery surface coatings are 74.9%, slightly lower than 84.7% of the cell-only group (control) and 87.4% of the PDMS group. For the long-term culture, PDMS with slippery surface coatings has 83.9% of live cells, comparable with that of the cell-only group (88.6%) and slightly higher than that of the PDMS group (77.8%). These results further support the biocompatibility of the slippery surface coatings.

CONCLUSION

We demonstrate that the liquid-like slippery coating significantly reduces the adsorptions of proinflammatory serum proteins, human fibrinogen and albumin, on planar PDMS surfaces and in 3D microfluidic channels. The preparation of the surface coating relies on scalable and simple dip-coating methods. UV−vis spectra reveal the optical transparency of the surface coating, thereby enabling potential applications in optoelectronic devices. Additionally, MTT data show that the surface coating has good biocompatibility as PDMS and cell-only coculture systems with iNPCs. In addition, both short-term (7 days) and long-term (21 days) studies by live and dead assay show good cell viability of the prepared surface coatings. These results lay a foundation for the future applications of slippery surface coatings to reduce protein adsorptions for basic biomedical research and clinical medicine.

https://doi.org/10.1021/acsami.2c20834
ACS Appl. Mater. Interfaces 2023, 15, 9987−9995

EXPERIMENTAL SECTION

Materials. 2-Propanol (≥99.5%), sulfuric acid (95%−98%), dimethyldimethoxysilane (95%), agarose, Dulbecco's phosphate-buffered saline (PBS) with $MgCl_2$ and $CaCl_2$, 100 mL of a sodium bicarbonate solution (7.5%), poly(methyl methacrylate) (PMMA), Accutase solution, LDN193189 (a bone morphogenetic protein inhibitor), SB431542 (a transforming growth factor inhibitor), 3-(4,5-dimethyl-2-thiazolyl)-2,5-diphenyl-2*H*-tetrazolium bromide (MTT), and 98% retinoic acid (RA) were purchased from Sigma-Aldrich (St. Louis, MO). Poly(dimethylsiloxane) (PDMS; Dow SYLGARD 184) was purchased from Ellsworth Adhesives (Germantown, WI). Fluorescein-conjugated bovine serum albumin (BSA−FITC conjugate), fibrinogen from human plasma (Alexa Fluor 594 Conjugate), minimum essential medium-alpha (α-MEM), and Dulbecco's modified eagle medium (DMEM/F12) were received from Thermo Fisher Scientific (Waltham, MA). mTeSRTM 1 medium (20 mL of mTeSRTM 1 basal and 5 mL of mTeSRTM 1 5× supplement) was purchased from STEMCELL Technology, Inc. (Cambridge, MA). B-27 serum-free supplement, fibroblast growth factor-2 (FGF2), and penicillin/streptomycin were purchased from Life Technologies (Carlsbad, CA). Fetal bovine serum was purchased from Atlanta Biologicals (Lawrenceville, GA). Y27632 (a Rho-associated kinase inhibitor) was purchased from iXCells, Biotechnologies (San Diego, CA). Growth-factor-reduced Matrigel, a 150 mm tissue culture Petri dish, 24- and 96-well ultralow attachments, and 6-, 24-, and 96-well tissue culture plates were purchased from Corning (Corning, NY). Silicon wafers were bought from University Wafers. Ultrapure water applied in all of the washing steps was run by a Milli-Q Type 1 system.

Preparation and Characterization of Slippery Surface Coatings on PDMS Surfaces. PDMS thin films (thickness: ∼40 μm) were prepared by spin-coating silicone elastomers (elastomer/curing agent ratio, 10:1; Sylgard 184, Dow Corning) at 2000 rpm for 30 s on a PMMA-coated silicon wafer. The prepared PDMS thin films were then cured in a 75 °C oven for 1 h and treated with oxygen plasma (Harrick Plasma Inc.). In parallel, 2-propanol, dimenthyldimethoxysilane, and sulfuric acid were added to a 20 mL glass vial to prepare the reaction solution; the volume ratio of 2-propanol to dimenthyldimenthoxysilane to sulfuric acid was kept at 100:10:1. Next, the oxygen-plasma-treated PDMS thin films were dip-coated in the reactive solution for ∼30−60 s and then dried at room temperature or at 75 °C in an oven.

UV−Vis Spectra and Transparency Tests. The transparency of PDMS thin films with and without slippery surface coatings was measured by using a V-770 UV−vis/near-IR spectrophotometer (Easton, MD) under a wavelength range from 100 to 900 nm.

XPS Measurements. A Thermo Scientific K-Alpha X-ray photoelectron spectrometer was used to characterize the PDMS thin films with oxygen plasma treatments (n = 3) and three samples functionalized with the slippery surface coating.

Characterization of the Antiprotein Adsorption Property on Planar PDMS Surfaces. A total of 5 mg of BSA powder (FITC conjugate) was dissolved in Dulbecco's PBS to prepare a 1 mg/mL BSA-rich solution. Similarly, 5 mg of human fibrinogen powder (Alexa Fluor 594 Conjugate) was dissolved in a sodium bicarbonate solution to make a solution containing fibrinogen. The PDMS thin films treated with and without surface coatings on the silicon wafer were incubated in glass vials containing the BSA or human fibrinogen solution at 37 °C for 1, 3, 7, 14, 21, and 30 days, respectively. A Nikon A1R HD confocal microscope was used to capture high-resolution confocal images at excitation wavelengths of 488 nm (for BSA) and 558 nm (for fibrinogen).

Characterization of the Antiprotein Adsorption Property on 3D PDMS Microfluidic Channels. 3D PDMS microfluidic channels (cross section width, 200 μm; height, 50 μm) were prepared by using standard soft lithography and a molding process on a SU-8 mold. The above-mentioned reactive solution was pumped into oxygen-plasma-treated channels for 10 min to form the slippery surface coatings. The functionalized 3D microfluidic channels were then rinsed with DI water several times and dried in a 75 °C oven. Characterization of the antiprotein adsorption property started by infusing a protein-rich solution (1 mg/mL BSA in 1× PBS or 1 mg/mL fibrinogen in a sodium bicarbonate solution) with a flow rate at 1 μL/min into microfluidic channels that connected with a plastic tube. Confocal images were captured at 0, 5, 10, 15, and 20 min. Z-stack scanning (150 μm in total, with each step of 10 μm) was performed at a scanning speed of 1.56 s/step. Repeated experiments were performed at least three times for each group.

hiPSC Culture. The culture of hiPSCs was performed following our previous publications.[39,40] Human iPSK3 cells were derived from human foreskin fibroblast transfected with plasmid DNA encoding reprogramming factors OCT4, NANOG, SOX2, and LIN28. Briefly, the 6-well tissue culture plate was coated with Matrigel (1:30 dilution in DMEM/F12) and incubated at 37 °C. The cells were dissociated by Accutase for 5−10 min at 37 °C. Then, 1.5×10^6 cells were seeded onto the Matrigel-coated 6-well plate in the presence of 10 μM Y-27632 in a mTESR medium. The medium was changed every day, and the cells were passaged once a week.

Cortical Spheroid Differentiation from hiPSCs. The cortical spheroid differentiation was performed as shown in our previous publications.[41,42] Briefly, the dissociated hiPSCs were seeded into an ultralow attachment 24-well plate at 3×10^5 cells/well in the differentiation medium (DMEM/F12 + 2% B-27) and 10 μM Y-27632. After 24 h of incubation, the culture medium was changed to DMEM/F12/2% B27 with 10 μM SB431542 (a potent and selective inhibitor of the transforming growth factor-β pathway) and 100 nM LDN193189 (a potent inhibitor of the bone morphogenetic pathway). The medium was changed every other day. On day 8, the medium was changed to DMEM/F12/2% B-27 with 10 ng/mL FGF2 and 5 μM RA. This culture was maintained for another 8 days. The formed cortical spheroids were then replated onto Matrigel-coated surfaces until the neural network was established (around 10 days). This cell population was referred to as hiPSC-derived iNPCs.

MTT Assay for Biocompatibility Study. For a short-term biocompatibility study, the day-16 iNPCs were replated to the 96-well tissue culture plate containing PDMS with the slippery surface coating in neural differentiation medium. There are three groups used for comparison of the MTT activity. PDMS and cell-only conditions were tested as the control groups. The cells were incubated with a 5 mg/mL MTT solution at days 1, 3, 5, and 7 for 2−4 h. Then, the formazan crystals were centrifuged and hydrolyzed by dimethyl sulfoxide (Sigma). Afterward, the pink solution was read at 570 nm by the microplate reader (BioRad Laboratories, Hercules, CA).

Live/Dead Assay Analyzed by Two-Color Flow Cytometry. The cell viability of PDMS with or without coatings in the coculture system was determined using the Live/Dead staining kit (Molecular Probes) according to the manufacturer's protocol. For the short-term biocompatibility study, after a 7-day culture, the replated iNPCs were dissociated by Accutase for 40 min to make single-cell solutions. For the long-term biocompatibility study with neural cells, after a 21-day coculture, iNPCs were dissociated by Accutase for 40 min to make single-cell solutions. Then, 50 μM calcein AM and 2 mM ethidium homodimer-1 were added to the cell suspensions. The cells were incubated for 15−20 min at room temperature, protected from light. The stained cells were acquired by a BD FACSCanto II flow cytometer using 488 nm excitation and measuring green fluorescence emission for calcein (i.e., 530/30 bandpass) and red fluorescence emission for ethidium homodimer-1 (i.e., 610/20 bandpass) within 1−2 h. The acquired events were analyzed with proper color compensation against negative controls using *FlowJo* software.

Statistical Analysis. A Student's t test was used for statistical analysis of the protein adsorption experiments. A one-way analysis of variance (ANOVA) was conducted to compare the cell viabilities by MTT assay. All groups were compared with each other with Tukey's multiple comparisons test. *ImageJ* software was utilized to calculate and fully interpret the intensity of the fluorescence signals.

https://doi.org/10.1021/acsami.2c20834
ACS Appl. Mater. Interfaces 2023, 15, 9987−9995

■ ASSOCIATED CONTENT

Data Availability Statement

All data needed to evaluate the conclusions in the paper are present in the paper and/or the Supporting Information.

Supporting Information

The Supporting Information is available free of charge at https://pubs.acs.org/doi/10.1021/acsami.2c20834.

Advantages and limitations of various surface coatings (Table S1), quantitative fluorescence intensity analysis of planar PDMS surfaces with and without the slippery coating (Table S2), quantitative fluorescence intensity analysis of 3D microfluidic channels with and without the slippery coating (Table S3), XPS spectra of the slippery surface coating on PDMS (Figure S1), effects of active chemical solutions and treatments on the wetting properties of PDMS surfaces (Figure S2), speed-dependent friction coefficients under a constant load force of 1 N for PDMS surfaces with and without the slippery surface coating (Figure S3), antiprotein adsorption property of planar PDMS surfaces without coating and with the coating after mechanical treatments (Figure S4), and quantitative analysis of the average fluorescence intensity of protein removal as a function of time for microfluidic channels with and without the surface coating (Figure S5) (PDF)

Movie S1 of the mobility of water droplets on PDMS surfaces with a slippery coating at a tilt angle of 15° (MOV)

Movie S2 of the mobility of water droplets on bare PDMS surfaces at a tilt angle of 15° (MOV)

■ AUTHOR INFORMATION

Corresponding Authors

Yi Zhang − *Department of Biomedical Engineering and the Institute of Materials Science, University of Connecticut, Storrs, Connecticut 06269, United States;* orcid.org/0000-0002-0907-663X; Email: yi.5.zhang@uconn.edu

Yan Li − *Department of Chemical and Biomedical Engineering, FAMU-FSU College of Engineering, Florida State University, Tallahassee, Florida 32306, United States*; Email: yli@eng.famu.fsu.edu

Authors

Yue Cao − *Department of Biomedical Engineering and the Institute of Materials Science, University of Connecticut, Storrs, Connecticut 06269, United States*

Xingchi Chen − *Department of Chemical and Biomedical Engineering, FAMU-FSU College of Engineering, Florida State University, Tallahassee, Florida 32306, United States*

Avi Matarasso − *Department of Bioengineering, University of Washington, Seattle, Washington 98195, United States*

Zizheng Wang − *Department of Materials Science and Engineering and the Institute of Materials Science, University of Connecticut, Storrs, Connecticut 06269, United States*

Yang Song − *Department of Biomedical Engineering and the Institute of Materials Science, University of Connecticut, Storrs, Connecticut 06269, United States;* orcid.org/0000-0003-0626-0850

Guangfu Wu − *Department of Biomedical Engineering and the Institute of Materials Science, University of Connecticut, Storrs, Connecticut 06269, United States*

Xincheng Zhang − *Department of Biomedical Engineering and the Institute of Materials Science, University of Connecticut, Storrs, Connecticut 06269, United States*

He Sun − *Department of Biomedical Engineering and the Institute of Materials Science, University of Connecticut, Storrs, Connecticut 06269, United States;* orcid.org/0000-0003-3701-9453

Xueju Wang − *Department of Materials Science and Engineering and the Institute of Materials Science, University of Connecticut, Storrs, Connecticut 06269, United States;* orcid.org/0000-0002-0669-8759

Michael R. Bruchas − *Department of Bioengineering, Department of Anesthesiology and Pain Medicine, Center for Neurobiology of Addiction, Pain, and Emotion, and Department of Pharmacology, University of Washington, Seattle, Washington 98195, United States*

Complete contact information is available at: https://pubs.acs.org/10.1021/acsami.2c20834

Author Contributions

†These authors contributed equally.

Notes

The authors declare no competing financial interest.

■ ACKNOWLEDGMENTS

This work is supported by the University of Connecticut start-up fund, NIH RF1NS118287, and R01MH128721. The content is solely the responsibility of the authors and does not necessarily represent the official views of the National Institutes of Health. Partial support was received from the National Science Foundation (CBET 1917618). The authors are also thankful for support by the Florida State University Flow Cytometry Core facility.

■ REFERENCES

(1) Teo, A. J. T.; Mishra, A.; Park, I.; Kim, Y. J.; Park, W. T.; Yoon, Y. J. Polymeric Biomaterials for Medical Implants and Devices. *ACS Biomater Sci. Eng.* **2016**, *2* (4), 454−472.

(2) Doloff, J. C.; Veiseh, O.; de Mezerville, R.; Sforza, M.; Perry, T. A.; Haupt, J.; Jamiel, M.; Chambers, C.; Nash, A.; Aghlara-Fotovat, S.; et al. The Surface Topography of Silicone Breast Implants Mediates the Foreign Body Response in Mice, Rabbits and Humans. *Nat. Biomed Eng.* **2021**, *5* (10), 1115−1130.

(3) McLaughlin, K.; Jones, B.; Mactier, R.; Porteus, C. Long-Term Vascular Access for Hemodialysis Using Silicon Dual-Lumen Catheters with Guidewire Replacement of Catheters for Technique Salvage. *Am. J. Kidney Dis* **1997**, *29* (4), 553−559.

(4) Lloyd, A. W.; Faragher, R. G. A.; Denyer, S. P. Ocular Biomaterials and Implants. *Biomaterials* **2001**, *22* (8), 769−785.

(5) Zhu, Y.; Li, S.; Li, J.; Falcone, N.; Cui, Q.; Shah, S.; Hartel, M. C.; Yu, N.; Young, P.; de Barros, N. R.; et al. Lab-on-a-Contact Lens: Recent Advances and Future Opportunities in Diagnostics and Therapeutics. *Adv. Mater.* **2022**, *34* (24), 2108389.

(6) Filippi, M.; Buchner, T.; Yasa, O.; Weirich, S.; Katzschmann, R. K. Microfluidic Tissue Engineering and Bio-Actuation. *Adv. Mater.* **2022**, *34* (23), 2108427.

(7) Koh, A.; Kang, D.; Xue, Y.; Lee, S.; Pielak, R. M.; Kim, J.; Hwang, T.; Min, S.; Banks, A.; Bastien, P.; et al. A Soft, Wearable Microfluidic Device for the Capture, Storage, and Colorimetric Sensing of Sweat. *Sci. Transl Med.* **2016**, *8* (366), 366ra165.

(8) Zhang, Y.; Guo, H.; Kim, S. B.; Wu, Y.; Ostojich, D.; Park, S. H.; Wang, X.; Weng, Z.; Li, R.; Bandodkar, A. J.; et al. Passive Sweat Collection and Colorimetric Analysis of Biomarkers Relevant to Kidney Disorders Using a Soft Microfluidic System. *Lab Chip* **2019**, *19* (9), 1545−1555.

(9) Huang, X.; Li, J.; Liu, Y.; Wong, T.; Su, J.; Yao, K.; Zhou, J.; Huang, Y.; Li, H.; Li, D.; et al. Epidermal Self-Powered Sweat Sensors for Glucose and Lactate Monitoring. *Bio-Des Manuf* **2022**, *5* (1), 201−209.
(10) Zhang, Y.; Mickle, A. D.; Gutruf, P.; McIlvried, L. A.; Guo, H.; Wu, Y.; Golden, J. P.; Xue, Y.; Grajales-Reyes, J. G.; Wang, X.; et al. Battery-Free, Fully Implantable Optofluidic Cuff System for Wireless Optogenetic and Pharmacological Neuromodulation of Peripheral Nerves. *Sci. Adv.* **2019**, *5* (7), eaaw5296.
(11) Zhang, Y.; Castro, D. C.; Han, Y.; Wu, Y.; Guo, H.; Weng, Z.; Xue, Y.; Ausra, J.; Wang, X.; Li, R.; et al. Battery-Free, Lightweight, Injectable Microsystem for in Vivo Wireless Pharmacology and Optogenetics. *Proc. Natl. Acad. Sci. U. S. A.* **2019**, *116* (43), 21427−21437.
(12) Wu, G.; Heck, I.; Zhang, N.; Phaup, G.; Zhang, X.; Wu, Y.; Stalla, D. E.; Weng, Z.; Sun, H.; Li, H.; et al. Wireless, Battery-Free Push-Pull Microsystem for Membrane-Free Neurochemical Sampling in Freely Moving Animals. *Sci. Adv.* **2022**, *8* (8), eabn2277.
(13) Kozai, T. D.; Jaquins-Gerstl, A. S.; Vazquez, A. L.; Michael, A. C.; Cui, X. T. Brain Tissue Responses to Neural Implants Impact Signal Sensitivity and Intervention Strategies. *ACS Chem. Neurosci.* **2015**, *6* (1), 48−67.
(14) Eles, J. R.; Vazquez, A. L.; Kozai, T. D. Y.; Cui, X. T. Meningeal Inflammatory Response and Fibrous Tissue Remodeling around Intracortical Implants: An in Vivo Two-Photon Imaging Study. *Biomaterials* **2019**, *195*, 111−123.
(15) Maan, A. M. C.; Hofman, A. H.; Vos, W. M.; Kamperman, M. Recent Developments and Practical Feasibility of Polymer-Based Antifouling Coatings. *Adv. Funct Mater.* **2020**, *30* (32), 2000936.
(16) McVerry, B.; Polasko, A.; Rao, E.; Haghniaz, R.; Chen, D.; He, N.; Ramos, P.; Hayashi, J.; Curson, P.; Wu, C. Y.; et al. A Readily Scalable, Clinically Demonstrated, Antibiofouling Zwitterionic Surface Treatment for Implantable Medical Devices. *Adv. Mater.* **2022**, *34* (20), 2200254.
(17) Bjugstad, K. B.; Redmond, D. E., Jr.; Lampe, K. J.; Kern, D. S.; Sladek, J. R., Jr.; Mahoney, M. J. Biocompatibility of PEG-Based Hydrogels in Primate Brain. *Cell Transplant* **2008**, *17* (4), 409−415.
(18) Lynn, A. D.; Blakney, A. K.; Kyriakides, T. R.; Bryant, S. J. Temporal Progression of the Host Response to Implanted Poly-(Ethylene Glycol)-Based Hydrogels. *J. Biomed Mater. Res. A* **2011**, *96A* (4), 621−631.
(19) Browning, M. B.; Cereceres, S. N.; Luong, P. T.; Cosgriff-Hernandez, E. M. Determination of the in Vivo Degradation Mechanism of PEGDA Hydrogels. *J. Biomed Mater. Res. A* **2014**, *102* (12), 4244−4251.
(20) Golabchi, A.; Wu, B.; Cao, B.; Bettinger, C. J.; Cui, X. T. Zwitterionic Polymer/Polydopamine Coating Reduce Acute Inflammatory Tissue Responses to Neural Implants. *Biomaterials* **2019**, *225*, 119519.
(21) Erathodiyil, N.; Chan, H.-M.; Wu, H.; Ying, J. Y. Zwitterionic Polymers and Hydrogels for Antibiofouling Applications in Implantable Devices. *Mater. Today* **2020**, *38*, 84−98.
(22) Yang, Q.; Wu, B.; Eles, J. R.; Vazquez, A. L.; Kozai, T. D. Y.; Cui, X. T. Zwitterionic Polymer Coating Suppresses Microglial Encapsulation to Neural Implants in Vitro and in Vivo. *Adv. Biosyst* **2020**, *4* (6), 1900287.
(23) Chan, D.; Chien, J.-C.; Axpe, E.; Blankemeier, L.; Baker, S. W.; Swaminathan, S.; Piunova, V. A.; Zubarev, D. Y..; Maikawa, C. L.; Grosskopf, A. K.; Mann, J. L.; Soh, H. T.; Appel, E. A. Combinatorial Polyacrylamide Hydrogels for Preventing Biofouling on Implantable Biosensors. *Adv. Mater.* **2022**, *34*, 2109764.
(24) Leslie, D. C.; Waterhouse, A.; Berthet, J. B.; Valentin, T. M.; Watters, A. L.; Jain, A.; Kim, P.; Hatton, B. D.; Nedder, A.; Donovan, K.; et al. A Bioinspired Omniphobic Surface Coating on Medical Devices Prevents Thrombosis and Biofouling. *Nat. Biotechnol.* **2014**, *32* (11), 1134−1140.
(25) Sun, H.; Li, R.; Li, H.; Weng, Z.; Wu, G.; Kerns, P.; Suib, S.; Wang, X.; Zhang, Y. Bioinspired Oil-Infused Slippery Surfaces with Water and Ion Barrier Properties. *ACS Appl. Mater. Interfaces* **2021**, *13* (28), 33464−33476.
(26) Han, K.; Wang, Z.; Heng, L.; Jiang, L. Photothermal Slippery Surfaces Towards Spatial Droplet Manipulation. *J. Mater. Chem. A* **2021**, *9* (31), 16974−16981.
(27) Guo, P.; Wang, Z.; Heng, L.; Zhang, Y.; Wang, X.; Jiang, L. Magnetocontrollable Droplet and Bubble Manipulation on a Stable Amphibious Slippery Gel Surface. *Adv. Funct Mater.* **2019**, *29* (11), 1808717.
(28) Lee, Y.; Shin, H.; Lee, D.; Choi, S.; Cho, I. J.; Seo, J. A Lubricated Nonimmunogenic Neural Probe for Acute Insertion Trauma Minimization and Long-Term Signal Recording. *Adv. Sci.* **2021**, *8* (15), 2100231.
(29) Sett, S.; Yan, X.; Barac, G.; Bolton, L. W.; Miljkovic, N. Lubricant-Infused Surfaces for Low-Surface-Tension Fluids: Promise Versus Reality. *ACS Appl. Mater. Interfaces* **2017**, *9* (41), 36400−36408.
(30) Wang, Z.; Xu, Q.; Wang, L.; Heng, L.; Jiang, L. Temperature-Induced Switchable Interfacial Interactions on Slippery Surfaces for Controllable Liquid Manipulation. *J. Mater. Chem. A* **2019**, *7* (31), 18510−18518.
(31) Wang, X.; Wang, Z.; Heng, L.; Jiang, L. Stable Omniphobic Anisotropic Covalently Grafted Slippery Surfaces for Directional Transportation of Drops and Bubbles. *Adv. Funct Mater.* **2020**, *30* (1), 1902686.
(32) Wu, Q.; Yang, C.; Su, C.; Zhong, L.; Zhou, L.; Hang, T.; Lin, H.; Chen, W.; Li, L.; Xie, X. Slippery Liquid-Attached Surface for Robust Biofouling Resistance. *ACS Biomater Sci. Eng.* **2020**, *6* (1), 358−366.
(33) Wang, L.; McCarthy, T. J. Covalently Attached Liquids: Instant Omniphobic Surfaces with Unprecedented Repellency. *Angew. Chem. Int. Ed* **2016**, *55* (1), 244−248.
(34) Lu, L.; Gutruf, P.; Xia, L.; Bhatti, D. L.; Wang, X.; Vazquez-Guardado, A.; Ning, X.; Shen, X.; Sang, T.; Ma, R.; et al. Wireless Optoelectronic Photometers for Monitoring Neuronal Dynamics in the Deep Brain. *Proc. Natl. Acad. Sci. U. S. A.* **2018**, *115* (7), E1374−E1383.
(35) Shakeri, A.; Khan, S.; Didar, T. F. Conventional and Emerging Strategies for the Fabrication and Functionalization of PDMS-Based Microfluidic Devices. *Lab Chip* **2021**, *21* (16), 3053−3075.
(36) Tan, H. Y.; Cho, H.; Lee, L. P. Human Mini-Brain Models. *Nat. Biomed Eng.* **2021**, *5* (1), 11−25.
(37) Garreta, E.; Kamm, R. D.; Chuva de Sousa Lopes, S. M.; et al. Rethinking Organoid Technology through Bioengineering. *Nat. Mater.* **2021**, *20*, 145−155.
(38) Marzano, M.; Bou-Dargham, M. J.; Cone, A. S.; York, S.; Helsper, S.; Grant, S. C.; Meckes, D. G., Jr.; Sang, Q. A.; Li, Y. Biogenesis of Extracellular Vesicles Produced from Human-Stem-Cell-Derived Cortical Spheroids Exposed to Iron Oxides. *ACS Biomater Sci. Eng.* **2021**, *7* (3), 1111−1122.
(39) Yan, Y.; Bejoy, J.; Xia, J.; Guan, J.; Zhou, Y.; Li, Y. Neural Patterning of Human Induced Pluripotent Stem Cells in 3-D Cultures for Studying Biomolecule-Directed Differential Cellular Responses. *Acta Biomater* **2016**, *42*, 114−126.
(40) Yan, Y.; Song, L.; Madinya, J.; Ma, T.; Li, Y. Derivation of Cortical Spheroids from Human Induced Pluripotent Stem Cells in a Suspension Bioreactor. *Tissue Eng. Part A* **2018**, *24* (5−6), 418−431.
(41) Song, L.; Yuan, X.; Jones, Z.; Vied, C.; Miao, Y.; Marzano, M.; Hua, T.; Sang, Q. A.; Guan, J.; Ma, T.; et al. Functionalization of Brain Region-Specific Spheroids with Isogenic Microglia-Like Cells. *Sci. Rep* **2019**, *9* (1), 11055.
(42) Song, L.; Yuan, X.; Jones, Z.; Griffin, K.; Zhou, Y.; Ma, T.; Li, Y. Assembly of Human Stem Cell-Derived Cortical Spheroids and Vascular Spheroids to Model 3-D Brain-Like Tissues. *Sci. Rep* **2019**, *9* (1), 5977.

https://doi.org/10.1021/acsami.2c20834
ACS Appl. Mater. Interfaces 2023, 15, 9987−9995